

Preliminary Analysis of the Cladding Mechanical Behavior of a Nuclear Superheat Boiling Water Reactor

Majid Bahonar

Department of Nuclear Engineering,
Science and Research branch, Islamic Azad University, Tehran, Iran.
E-mail: majid_bhnr@yahoo.com

Gholamreza Jahanfarnia*

Department of Nuclear Engineering,
Science and Research branch, Islamic Azad University, Tehran, Iran.
E-mail: rezajahan@yahoo.com

*Corresponding author

Morteza Gharib

Department of Nuclear Engineering,
Science and Research branch, Islamic Azad University, Tehran, Iran.
E-mail: mgharib2@yahoo.com

Received: 30 January 2018, Revised: 19 February 2018, Accepted: 7 May 2018

Abstract: In the present study, investigation of mechanical behaviour of the fuel cladding material for a nuclear superheat Boiling Water Reactor with annular fuel rods, is carried out. In this design, each annular fuel element is cooled internally by steam and externally by water. For the fuel cladding material, radiation embrittlement and irradiation-assisted stress corrosion cracking (IASCC) are the most important issues that have to be taken into account. Hence, for cladding, two materials are considered. Preliminary thermal expansion and stress analysis have been done for a fresh (begin of cycle) ASBWR (Annular-fuelled Superheat Boiling Water Reactor) fuel element. The purpose of these analysis is to investigate the stress distribution and thermal expansion of the cladding in the initial phase of operation. The results show that there is a noticeable difference in the axial expansion between the inner and outer claddings. For T91 (modified 9Cr-1Mo steel) cladding, the maximum axial thermal growth of the inner cladding is 22.12 mm, which is about 9.7 mm more than the outer cladding. For Inconel 718 cladding, the results are 27.8 mm and 13.4 mm, respectively.

Keywords: Annular fuel, Strain, Stress, Superheat BWR, Thermal expansion

Reference: Bahonar, M., Jahanfarnia, Gh., and Gharib, M., "Preliminary Analysis of the Cladding Mechanical Behavior of a Nuclear Superheat Boiling Water Reactor", Int J of Advanced Design and Manufacturing Technology, Vol. 11/No. 2, 2018, pp. 39-45.

Biographical notes: **Majid Bahonar** received his PhD in Nuclear Engineering from IAU, Science and Research Branch, in 2017. His research interests include power plant technology, Reactor thermal-hydraulic and safety analysis, and two phase flow. **Gholamreza Jahanfarnia** received his PhD in Nuclear Power Plant from University of Moscow, in 2005. He is currently Professor at the Department of Nuclear Engineering, science and research branch University, Tehran, Iran. His current research interest includes power plant technology and two phase flow. **Morteza Gharib** is Associate Professor of Nuclear engineering at the Amirkabir University and IAU, Iran. He received his PhD in Nuclear engineering from Pennsylvania University of USA.

1 INTRODUCTION

A selection of available and promising materials for reactor in-core components is based on their mechanical and nuclear properties, corrosion and creep fracture resistance, irradiation stability and manufacturing feasibility. Particularly for the fuel cladding material in a nuclear reactor, radiation embrittlement and irradiation-assisted stress corrosion cracking (IASCC) are the most important issues that have to be taken into account.

Superheating can be incorporated in nuclear power plants by the addition of either a nuclear or fossil fuel-fired super heater. Nuclear super heaters can be further categorized into two types: (a) the separate or non-integral nuclear super heater and (b) the integral nuclear super heater [1]. The non-integral nuclear super heater is namely a steam-cooled reactor. It only adds superheat to steam and the steam coolant is supplied from other sources, such as a light water reactor (LWR) or fossil power plant. For integral nuclear super heater, steam is generated and superheated by using the same core. Although the reactor design will be more complicated, it is believed that the integral nuclear super heater is more cost-effective than the separate one because it needs only one core and one reactor pressure vessel to produce superheated steam. It is essential to use advanced materials for the in-core and out-of-core structures. The in-core structures, such as fuel cladding, are the most critical components in the pressure vessel, as they are exposed to the highest service temperature, to severe irradiation dose, and to the oxidizing superheated steam environment. The desirable characteristics of the in-core materials include good mechanical strength at high temperatures, resistance to radiation damage and corrosion, low neutron absorption cross section and good heat transfer properties.

In order to take advantage of the abundant experience from today's light water reactors, as well as improve the LWR technology, this study evaluates mechanical behavior of the fuel-cladding design of an integral nuclear super heater cooled by water and steam. In this paper, a mechanical analysis of a superheat BWR fuel-cladding in steady state conditions is carried out. Through a preliminary study, two materials are considered to have the potential to fulfill the requirements as in-core cladding and structural materials in the ASBWR.

2 METHODS AND RESULTS

In each fuel assembly for proposed design by YU-Chi KO [2], water is heated by the outer surface of the annular fuel elements and the steam-water or two-phase mixture is formed through the heating paths (or sub-channels). The two-phase mixture, composed of about

10 to 20% saturated steam, continues to flow upward and enters the annular separator and dryer, (Fig. 1 & Fig. 2). Annular separators and steam dryers are located above the core in the reactor vessel. The fuel assembly contains sixty annular fuel elements and one square water rod in an 8×8 square array. The steam coolant first flows downward to the 28 central fuel elements and enters a steam box at the bottom end of the fuel element and then, the steam coolant is redirected to the 32 peripheral fuel elements. The view of the steam box and proposed fuel assembly are shown in Fig. 3 and Fig. 4. The main design data is summarized in Table 1.

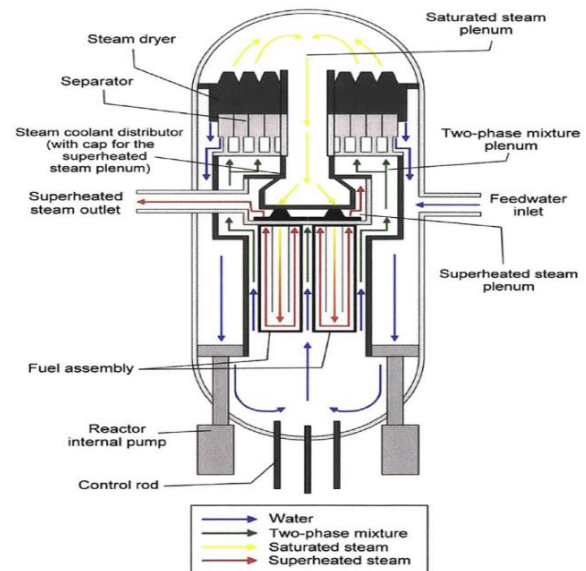


Fig. 1 Flow configuration of Superheat BWR by KO [2]

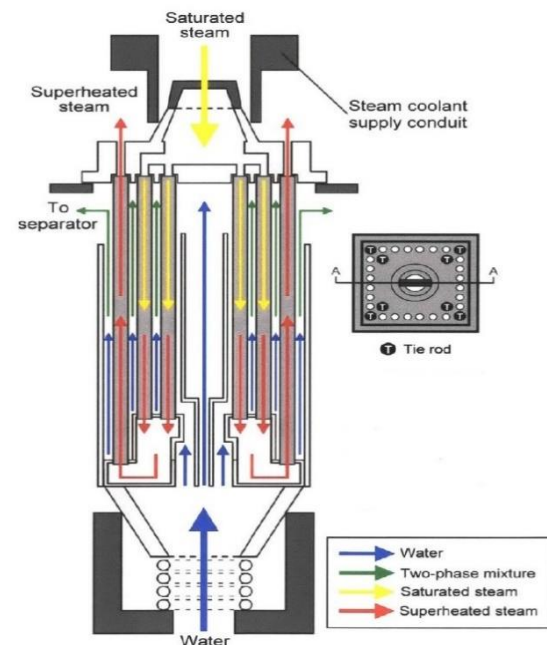


Fig. 2 A view of proposed fuel assembly [2]

Table 1 Superheat BWR design data

Parameters	Unit	Value
Reactor Thermal Power	MW	1250
System Pressure	bar	71.3
Fuel assembly average power	MW	6.5
No. of fuel assembly	-	192
Fuel material	-	UO2
Cladding material	-	T91/Inconel718
Fuel average enrichment	%	6-7
Fuel inside diameter	mm	10
cladding outside diameter	mm	19.6
Height of fuel rod	m	3
No. of Spacers	-	7
Pitch of fuel rods	mm	23
Assembly outer dimension	mm	193.7
Inlet mass flow rate	kg/s	16.3
Outlet steam temperature	°C	557.3
Efficiency	%	40

The heat transfer equation in cylindrical coordinate with boundary conditions are solved with fluid equations, (Fig.5 & Fig.6). The functions of steam box are collecting the incoming steam coolant; providing a mixing space for the steam coolant to reduce the local temperature peaking; and directing the steam coolant back to the peripheral up-flow fuel elements. It includes of the upper steam box and the lower steam box.

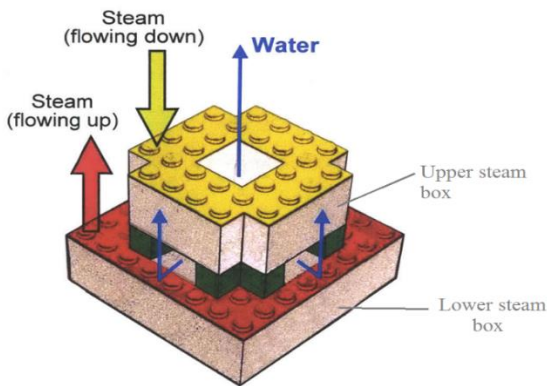


Fig. 3 A view of steam box

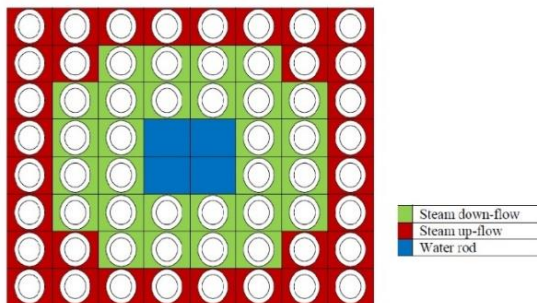


Fig. 4 Downward and upward regions in a fuel assembly

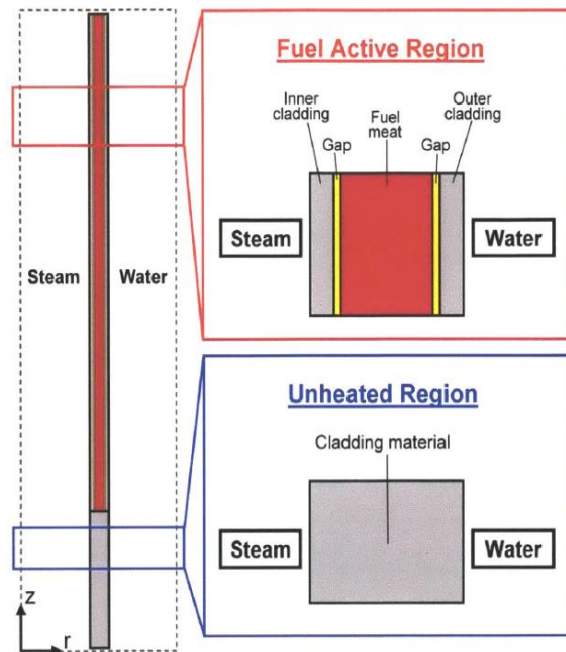


Fig. 5 Configuration of fuel element.

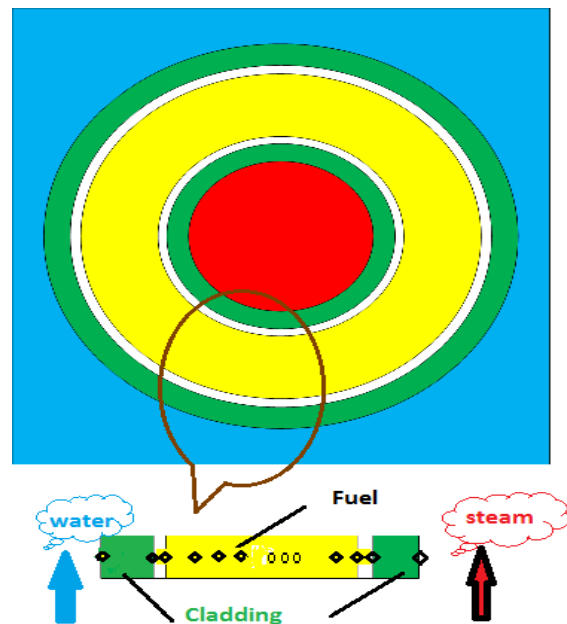


Fig. 6 Boundary conditions in a fuel element

The proposed design, should improve safety margins to that of the existing BWRs including a limitation on minimum critical power ratio, maximum fuel and cladding temperature. Furthermore, it is important to confirm that the advantages gained in higher thermal efficiency must not be lost through depreciating factors, such as lower allowable power density in the superheating region or excessively higher annular fuel fabrication costs.

For cladding material, the first candidate is the modified 9Cr-1Mo steel (T91). It is ferrites-martensitic steel currently used in fossil power plant super heaters. T91 has a lower thermal expansion coefficient compared to stainless steel and has excellent performance under 650°C. The potential of T91 for nuclear applications has been recently studied. It is considered as one of the promising structural materials for the lead-bismuth-cooled accelerator driven system (ADS) [3]. In addition, the feasibility of using T91 as fuel cladding in supercritical water reactors is also under investigation [4].

The second candidate is Inconel 718. It is a precipitation-hardenable nickel-chromium alloy containing significant amounts of iron, niobium, and molybdenum along with lesser amounts of aluminum and titanium. Inconel 718 combines excellent corrosion resistance and tensile, fatigue, creep, and rupture strength with outstanding weld ability, including resistance to post weld cracking. It has satisfactory performance when operated between 423 to 1300°F. Compared with stainless steel, Inconel 718 has improved ductile to brittle transition behavior under irradiation and thermal creep fracture resistance of the cladding during transients. In addition, Inconel 718 has been proposed as a cladding material for liquid metal and gas-cooled fast breeder reactors [5].

Table 2 Young's modulus of the cladding materials [6,7]

Temperature(°c)	Young modulus (GPa)	
	T91	Inconel718
20	206.0	201.2
100	199.5	197.5
200	194.4	192.2
300	187.9	186.3
400	181.5	179.7
500	175.0	172.4
600	151.0	164.4
700	127.0	155.8

Table 3 Linear thermal expansion coefficients of the cladding materials [6,7]

Temperature(°c)	Linear thermal expansion coefficient ($10^{-6} / K$)	
	T91	Inconel718
100	10.8	13.2
200	11.2	13.5
300	11.6	13.9
400	11.9	14.2
500	12.2	14.5
600	12.5	14.9
700	12.7	15.5

Preliminary thermal expansion and stress analyses have been done for a fresh ASBWR fuel element. The purpose of these analyses is to investigate the stress distribution and thermal expansion of the cladding in the initial phase

of operation. All assumptions applied to the analysis are listed in Table 2. Young's modulus and linear thermal expansion coefficients of the cladding materials are listed in Table 2 and Table 3, respectively [6,7].

Fig. 7 illustrates the pressure acting on the inner and outer cladding of the fresh fuel. Fig. 8 shows the force balance for calculation of the axial stresses.

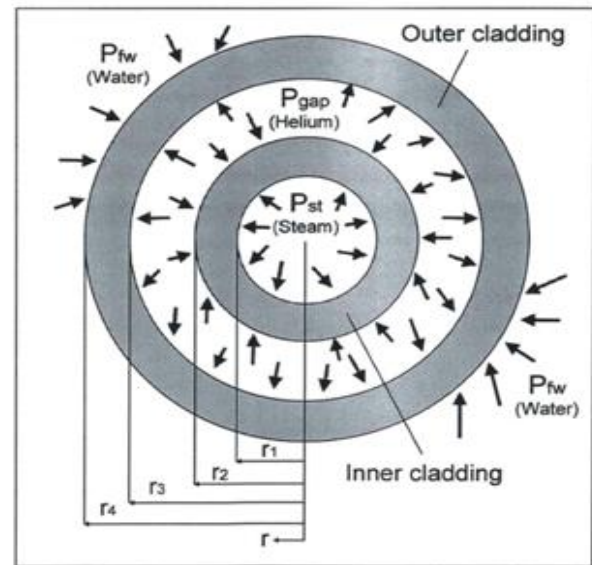


Fig. 7 Illustration of the pressures acting on cladding

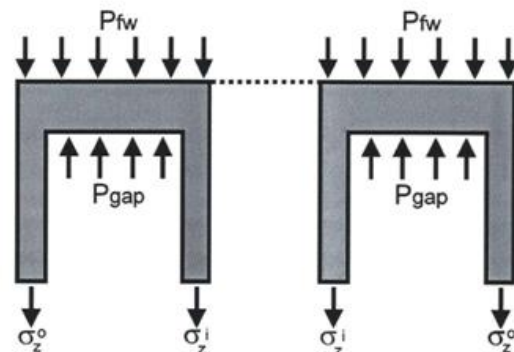


Fig. 8 Balance of the axial forces

Stresses caused by pressure can be expressed as the following equations [8].

For the inner cladding:

$$\sigma_r^i = \frac{-(P_{st} + P_{gap})}{2} \quad (1)$$

$$\sigma_\theta^i = \frac{r_1 P_{st} - r_2 P_{gap}}{r_2 - r_1} \quad (2)$$

$$\sigma_z^i = \frac{(r_3^2 - r_2^2)P_{gap} - (r_4^2 - r_1^2)P_{fw}}{(r_4^2 - r_3^2) + (r_2^2 - r_1^2)} \quad (3)$$

For the outer cladding:

$$\sigma_r^o = \frac{-(P_{fw} + P_{gap})}{2} \quad (4)$$

$$\sigma_\theta^o = \frac{r_3 P_{gap} - r_4 P_{fw}}{r_4 - r_3} \quad (5)$$

$$\sigma_z^o = \frac{(r_3^2 - r_2^2)P_{gap} - (r_4^2 - r_1^2)P_{fw}}{(r_4^2 - r_3^2) + (r_2^2 - r_1^2)} \quad (6)$$

Where the superscripts o, i, refer to outer and inner claddings respectively; Pst, Pgap and Pfw refer to steam, gap and water pressures, respectively, $\sigma_r^T, \sigma_\theta^T, \sigma_z^T$ refer to radial, hoop and axial stresses, respectively. Table 4 summarizes the calculation results. It can be found that the inner cladding is subject to tensile hoop stress while the outing is subject to compressive hoop stress at the beginning of cycle. However, after the fuel burn-up increases, the fuel internal pressure will increase considerably due to the release of fission gas from the fuel pellets. The plenum pressure will eventually be higher than the system pressure, and then the inner and outer claddings will be subject to compressive and tensile stresses, respectively.

If the wall of a long hollow cylinder is heated non-uniformly through its thickness, its elements would not expand uniformly and thermal stresses are induced due to this mutual interference. Considering the cladding structure as a long, hollow cylinder, its thermal stresses can be expressed as [8]:

$$\sigma_r^T = \frac{\alpha E}{(1-\nu)r^2} \left[\frac{r^2 - a^2}{b^2 - a^2} \int_a^b T(r)rdr - \int_a^r T(r)dr \right] \quad (7)$$

$$\sigma_\theta^T = \frac{\alpha E}{(1-\nu)r^2} \left[\frac{r^2 + a^2}{b^2 - a^2} \int_a^b T(r)rdr + \int_a^r T(r)dr - T(r)r^2 \right] \quad (8)$$

$$\sigma_z^T = \frac{\alpha E}{(1-\nu)} \left[\frac{2}{b^2 - a^2} \int_a^b T(r)rdr - T(r) \right] \quad (9)$$

Where the superscripts T refer to thermal stresses, α, ν and E are thermal expansion, Poisson ratio and Young's modulus, respectively, a and b are inner and outer radius, respectively. This analysis assumes the long cylinder to

be axially unconstrained. Fig. 9 shows the peak thermal stresses on the steam side (inner) cladding. The maximum radial thermal stress (σ_r^T) is about 1.33 MPa which is negligible compared to σ_θ^T and σ_z^T .

Fig. 10 shows the maximum thermal stresses on the water side (outer) of the cladding. Compared with Fig. 9, the water side cladding has slightly higher maximum thermal stresses because its radial temperature distribution is less uniform than that of the steam side cladding.

Table 4 Calculation results of the stresses caused by pressure at the beginning of fuel life

	σ_r (MPa)	σ_θ (MPa)	σ_z (MPa)
Inner cladding	-4.01	33.22	-19.82
Outer cladding	-4.29	-75.08	-19.82

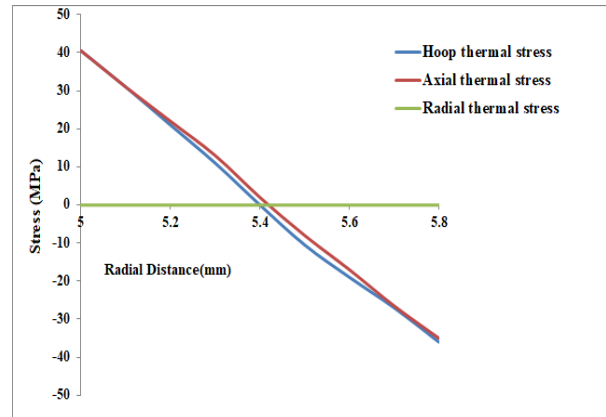


Fig. 9 Peak thermal stresses on the steam side (inner) cladding

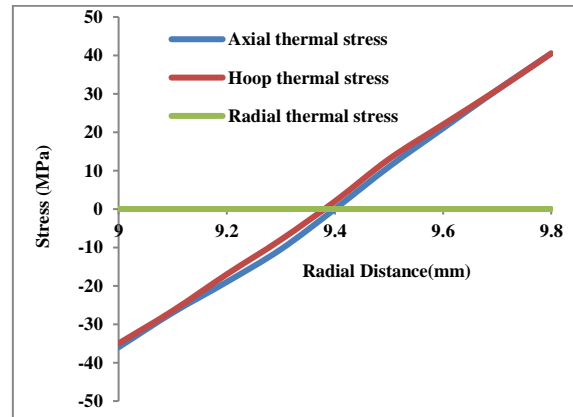


Fig. 10 Peak thermal stresses on the water side (outer) cladding

During plant operation, cladding deforms gradually due to pressure, thermal expansion and irradiation effects etc.

In this section, deformation of fresh fuel cladding caused by pressure and thermal expansion is evaluated. Strains caused by pressure and thermal expansion can be expressed as [8]:

$$\epsilon_r = \frac{1}{E} [\sigma_r - \nu(\sigma_z + \sigma_\theta)] + \int_{T_0}^T \alpha_r dT \quad (10)$$

$$\epsilon_\theta = \frac{1}{E} [\sigma_\theta - \nu(\sigma_z + \sigma_r)] + \int_{T_0}^T \alpha_\theta dT \quad (11)$$

$$\epsilon_z = \frac{1}{E} [\sigma_z - \nu(\sigma_r + \sigma_\theta)] + \int_{T_0}^T \alpha_z dT \quad (12)$$

Where $\epsilon_r, \epsilon_\theta, \epsilon_z$ are radial, hoop and axial strains, respectively; at reference temperature (20°C). In this evaluation, the cladding material is assumed to expand isotropically, therefore $\alpha_r = \alpha_\theta = \alpha_z = \alpha$. Table 5 summarizes the calculation results of strains, radial displacement, and axial and radial growths due to pressure and thermal expansion for the hot channel. The steam down-flowing and up-flow channels have different axial growths of the inner cladding since steam temperature is higher in the up-flow channels. For the axial growth of the outer cladding, the results between the steam down-flow and up-flow channels are about the same. Although the radial strain is about the same magnitude as the axial strain, the radial growth in cladding is very small due to the thin cladding thickness.

Table 5 Results of strain calculation of the base case (T91 cladding)

	Axial strain	Axial growth (mm)	Radial strain	Radial growth (mm)	Hoop strain
Inner cladding	0.0051	0.0055	0.0038	0.0046	16.16
Outer cladding	0.0038	0.0032	0.0031	0.0038	12.87
Inner cladding	0.0070	0.0074	0.0059	0.0075	21.41
Outer cladding	0.0039	0.0033	0.0031	0.0039	12.25

In addition, it can be seen from Table 5 that there is a noticeable difference in axial growth between the inner and outer claddings. For the steam up-flow channel, the axial growth of the inner cladding is 21.4 mm and is 12.25 mm for the outer cladding. The difference is about 1 cm. On the other hand, the difference in axial growth between the inner and outer claddings of the steam

down-flow channel is only 0.4 cm. Table 6 summarizes the calculation results of axial growth due to pressure and thermal expansion. Results of the average and hot channels are also compared. It is found that the results of axial growth between the average and hot channels are approximately within a difference of 2 mm. Furthermore, Inconel 718 has larger overall axial growth and larger difference in axial growth between the inner and outer claddings due to its higher thermal expansion coefficient. Given the power density of 50 kW/L, for Inconel 718 the maximum axial growth is 27.7 mm while for T91 it is 22.12 mm.

Table 6 Calculation Results of axial growth due to pressure and thermal expansion

			T91	Inconel718
			Axial growth(mm)	
Average channel	Steam down-flow	Inner cladding	15.81	19.02
		Outer cladding	12.11	14.52
	Steam up-flow	Inner cladding	20.33	25.74
		Outer cladding	12.92	15.00
Hot channel	Steam down-flow	Inner cladding	16.53	19.97
		Outer cladding	12.25	15.08
	Steam up-flow	Inner cladding	22.12	27.77
		Outer cladding	12.42	14.38

Table 7 shows the results of axial growth due to pressure and thermal expansion with various power densities.

Table 7 Impact of power density on the axial growth

Power density(kw/L)	T91	Inconel718	T91	Inconel718
	Maximum axial growth(mm)		Difference of axial growth between inner and outer claddings(mm)	
40	19.0	--	8.73	--
45	19.8	--	9.20	--
50	22.12	27.77	9.70	13.39
55	20.90	26.80	9.97	12.82
60	21.2	26.8	10.58	13.12
65	21.5	27.7	10.82	13.42
70	21.7	27.7	11.01	13.98
75	--	28.1	--	14.21
80	--	28.5	--	14.41

As shown in Table 7, as the power density increases, the overall axial growth and the difference in axial growth between the inner and outer claddings also increase. The overall axial growth is expected to be accommodated by the spring ends. The difference in axial growth between the inner and outer claddings is expected to be compensated by bellows.

3 CONCLUSION

In this study, a Preliminary analysis of the thermal expansion and stress distribution have been done for the fresh ASBWR fuel cladding. The results indicate that there is a noticeable difference in the axial expansion between the inner and outer claddings. For T91, the maximum axial thermal growth of the inner cladding is 22.12 mm, which is about 9.7 mm more than the outer cladding.

For Inconel 718, the results are 27.7 mm and 13.4 mm, respectively. The overall axial expansion is expected to be accommodated by springs at the fuel element upper end. The uneven axial expansion between the inner and outer claddings is expected to be compensated by bellows. Further studies are needed to investigate the long term fuel performance and the reliability of the proposed end springs and bellows.

REFERENCES

- [1] Novick, M., et al., Developments in Nuclear Superheat, Proceedings of the Third International Conference on the Peaceful Uses of Atomic Energy, Geneva, Aug. 31, Sep. 9, 1964.
- [2] Chih Ko, Yu., Conceptual Design of an Annular-Fueled Superheat Boiling Water Reactor, MIT Ph.D Thesis, Jun. 2010.
- [3] Sapundjiev, D., Al Mazouzi, A., and Van Dyck, S., A Study of the Neutron Irradiation Effects on the Susceptibility to Embrittlement of A316L and T91 Steels in Lead-Bismuth Eutectic, Journal of Nuclear Materials, Vol. 356, No. 1-3, Sep. 2006, pp. 229-236.
- [4] Chen, S., Sridharan, K., and Allen, T., Corrosion Behavior of Ferritic-Martensitic Steel T91 in Supercritical Water, Corrosion Science, Vol. 48, No. 9, 2006, pp. 2843-2854.
- [5] Fazzolae, R., Gas-Cooled Fast Breeder Reactor Designs with Advanced Fuel and Cladding, Nuclear Engineering and Design, Vol. 40, No. 1, Jan. 1977, pp. 191-201.
- [6] Inconel 718 Properties, On-line Resource, Available from World Wide Web:
<http://www.espimetals.com/tech/inconel718.pdf>
<http://www.espimetals.com/technicaldata.htm>
- [7] Ashrafi Nik, M., Dec. Thermo Hydraulic Optimization of the EURISOL DS Target, No. 2, TM-34-06-04, 2006.
- [8] Harvey, J. F., Theory and Design of Pressure Vessels, Springer, Sep. 1991.